

8669320

A REPORT FROM  
**OWENS-ILLINOIS**  
**TECHNICAL CENTER**



FORM NO. 605-K



CONSUMER & TECHNICAL PRODUCTS DIVISION  
RESEARCH, DEVELOPMENT & ENGINEERING

Reproduced by  
**NATIONAL TECHNICAL  
INFORMATION SERVICE**  
Springfield, Va. 22151

**OWENS-ILLINOIS**  
GENERAL OFFICES  TOLEDO 1, OHIO

SPONSORED BY:  
ADVANCED RESEARCH PROJECTS AGENCY  
ARPA ORDER NO. 1441  
PROGRAM CODE P9D10

SAT R-AD 728467

SEMI-ANNUAL TECHNICAL REPORT  
By: N. L. Boling, L. Spanoudis, and P. R. Wengert  
DAMAGE THRESHOLD STUDIES OF GLASS LASER MATERIALS

31 December 1971

CONTRACT NO. DAH15-~~68~~-C-0303  
69

CONTRACT DATE  
CONTRACT EXPIRATION  
CONTRACT AMOUNT

30 JUNE 1969  
30 JUNE 1972  
\$601,967



CONSUMER & TECHNICAL PRODUCTS DIVISION  
OWENS-ILLINOIS, INC.  
TOLEDO, OHIO

PHONE: (419) 242-6543, EXTENSION 33003

DISTRIBUTION STATEMENT A  
Approved for public release;  
Distribution Unlimited

## TABLE OF CONTENTS

1. Introduction. . . . .	1
2. Summary . . . . .	2
3. Melting Studies . . . . .	4
3.1 Mechanisms . . . . .	4
3.2 $\text{Ce}^{+3}/\text{Ce}^{+4}$ Ratio as a Measure of Oxygen Partial Pressure. . . . .	7
3.3 Melting Methods. . . . .	8
3.4 Remarks. . . . .	12
4. Laser For Damage Studies. . . . .	14
4.1 General. . . . .	14
4.2 Description of Laser . . . . .	14
Table 1 $\text{Ce}^{+3}/\text{Ce}^{+4}$ Equilibrium as a Measure of $P_{\text{O}_2}$ . . . . .	19
Table 2 Laser Glass Melts With Additions. . . . .	20
Table 3 Laser Glass Melts at Low $P_{\text{O}_2}$ . . . . .	21
Table 4 Effect of Remelting . . . . .	22
Figure 1 $\log (X_{\text{CeO}_2})^2/X_{\text{Ce}_2\text{O}_3}$ . . . . .	23
Figure 2 Oscillator . . . . .	24
Figure 3 Advantages of Long Rod Over Shorter Rod. . . . .	25
Figure 4 Oscillator-Amplifier System. . . . .	26
 Appendices	
I $\text{Ce}^{+3}/\text{Ce}^{+4}$ Equilibrium. . . . .	27
II Faraday Rotation in Nd:Glass Laser Systems . . . . .	28
References . . . . .	35
Figure Captions. . . . .	36

## 1. INTRODUCTION

The work being performed under this contract has the following three goals:

1. Development of a method for preventing the formation of damaging platinum particles in laser glass melted in platinum crucibles;
2. Design and construction of a high energy density glass laser operating in the TEM<sub>00</sub> mode.
3. Increasing the surface damage threshold of laser glass.

For (1) the main emphasis of the 1972 fiscal year is to reduce to practice the concept of melting laser glass under reduced oxygen partial pressure in order to continually obtain sparkler-free laser glass. A series of laser glass melts containing  $\text{Li}_2\text{O}$ ,  $\text{CaO}$ ,  $\text{SiO}_2$  and  $\text{Nd}_2\text{O}_3$  were made under various atmospheres, in different crucible materials and with additives, all with the intent of controlling the oxygen partial pressure within and over the melt.

The laser described in (2) above is very nearly in its final form.

Surface treatment studies are in progress and will be discussed in the next semi-annual report.

## 2. SUMMARY

The partial pressure of oxygen above a laser glass melt and the partial pressure of oxygen in equilibrium with the bulk melt itself have been found to be dramatic parameters controlling the total platinum content of laser glass and the occurrence of platinum sparklers. Using partial pressures of oxygen of  $10^{-10}$  atmospheres, laser glass was melted in platinum with a resultant platinum content of 0.017 to 0.033 ppm; this is more than two orders of magnitude lower than the 5ppm total platinum presently found in commercial melts.

The sparkler count within a laser glass sample was decreased from 19,200 sparklers per cubic inch to 18 per cubic inch by remelting the sample in a more oxidizing atmosphere than previously used. Laser damage threshold studies confirmed the orders of magnitude difference in sparkler count between the two samples.

Oxygen available during the initial melting of the batch material has been eliminated by several batch pretreatment methods.

Future efforts call for the integration of these findings in order to produce crucible melts of sparkler-free laser glass with a low concentration of total dissolved platinum.

The 30 nanosecond oscillator-amplifier system to be used in surface damage studies is complete, with the exception of a few minor modifications. An output of thirty-five joules in the TEM<sub>00</sub> mode has been obtained.

An optical shutter has been incorporated in the laser. This shutter will allow variation of the pulse width from 2-3 ns to 30-40 ns. Some work remains before this shutter is completely operational.

Surface treatments which might be effective in raising the surface damage threshold are currently under investigation. The results will be reported in the next semi-annual report.

### 3. MELTING STUDIES

#### 3.1 Mechanisms

Several mechanisms have been proposed for the introduction of platinum metal particles in laser glass. These mechanisms include 1) platinum metal vaporization, 2) platinum crucible attack by the molten glass or its vapors, 3) abrasion of platinum parts by the glass batch and the glass, and 4) platinum oxide vapor transport.

##### 3.1.1 Metal Vaporization

The vapor pressure of platinum metal at 1700°K is  $10^{-9.46}$  atm.<sup>(1)</sup> Under equilibrium conditions and assuming no diffusion of platinum metal into the glass, the platinum vaporized would be  $1.06 \times 10^{-8}$  g in the cover gas over the melt flowing at 5 CFH for 20 hours. If all this platinum were introduced, somehow into the melt (50 lb.), the platinum concentration would be  $4.66 \times 10^{-13}$  g/g or seven orders of magnitude less than what is normally found (about  $5 \times 10^{-8}$  g/g). A further argument against metal vapor transport is the ability to alter the platinum content of the glass by changing the oxygen partial pressure over the melt.

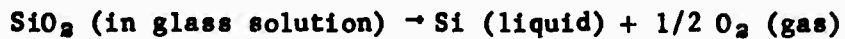
##### 3.1.2 Platinum Crucible Attack

When the oxygen partial pressure of the atmosphere over a laser glass melt is lowered, one would expect a point to be reached where

---

(1) A. S. Darling, "The Vapor Pressure of the Platinum Metals" Platinum Metals Review, 8 No. 4, (Oct. 1964)

the oxide components of the glass are destabilized, forming the free metal. For example:



The Si (liquid) would alloy with the platinum forming a low melting alloy. It has been speculated that the liquid alloy may migrate into the glass melt; leaving the platinum substrate and migrating into the melt would require an overall increase in surface energy and is highly unlikely. The silicon-platinum liquid alloy is therefore expected to remain in the grain boundaries until crucible failure occurs.

Glass melts were made at oxygen partial pressures as low as  $10^{-10}$  atmosphere with no evidence of crucible attack during this Report period. As a result, this mechanism of introducing platinum metal particles into laser glass is not proposed.

### 3.1.3 Crucible Abrasion

There have been observations made in certain platinum crucibles where grain growth has been substantially enhanced which indicate that the abrasion mechanism or a scaling or flaking mechanism may occur in very isolated, rare cases. The morphologies of the platinum particles and the crucible appearance of the vast majority of melt studies certainly does not indicate that crucible abrasion is an important mechanism, however.

#### 3.1.4 Vapor Phase Transport

The metallic inclusions found in laser glass have always taken the form of platelets, triangles, whiskers, etc., suggesting condensation from the vapor phase. Previously it had been believed that platinum vaporizes from the walls of the crucible as platinum metal or platinum oxide and is condensed on the glass surface, the platinum oxide decomposing to free platinum metal when it reaches the surface. Stirring of the melt would then mix the particles into the melt. Vapor phase transport (as described) is probably a significant mechanism for sparkler formation when the  $P_{O_2}$  is about 0.1 atmosphere or greater and when a potential gradient, such as a temperature gradient, is present.

#### 3.1.5 Solution - Dissolution

The present work suggests a slightly different mechanism of sparkler formation. It will be shown that the total platinum in the glass can be minimized by maintaining a low oxygen partial pressure over the melt during meltings. It will also be shown that when the melt and platinum crucible are exposed to a high oxygen partial pressure and then to a lower oxygen partial pressure (on a relative basis), a very large number of sparklers is produced as the  $PtO_2$  in the glass becomes a supersaturated solution. Finally, it will be shown that the number of sparklers can be remarkably decreased by exposing the melt to a higher oxygen partial pressure than it had seen during original melting.

The foregoing suggests that the platinum dissolves in the glass as an oxide or an oxide complex; for convenience, it can be thought of as  $\text{PtO}_2$  (in glass solution). The platinum remains dissolved or is precipitated as platinum sparklers depending upon the difference in oxygen partial pressure between the initial and final melting stages. This solution-dissolution mechanism is the most difficult of all of the proposed mechanisms to counteract because of the kinetics of treating the entire bulk of the glass.

### 3.2 $\text{Ce}^{+3}/\text{Ce}^{+4}$ Ratio as a Measure of Oxygen Partial Pressure

Cerium is the only multivalent component in laser glass containing  $\text{Li}_2\text{O}$ ,  $\text{CaO}$ ,  $\text{SiO}_2$  and  $\text{Nd}_2\text{O}_3$ . The  $\text{Ce}^{+3}/\text{Ce}^{+4}$  equilibrium therefore is a good indicator for determining the oxygen partial pressure in equilibrium with the bulk laser glass for any given set of parameters. Appendix 1 shows the thermodynamic derivation relating the cerium oxidation state of the glass to the oxygen partial pressure.

A number of melts have been made using a buffer gas which controlled the oxygen partial pressure above the melt. Although the intention was not to perform a detailed equilibrium study, the  $\text{Ce}_2\text{O}_3/\text{CeO}_2$  ratio can be related to the oxygen partial pressure if equilibrium is assumed. The summation of data is provided in Table 1. The  $P_{\text{O}_2}$  values are determined knowing the buffer gas mixture and assuming that equilibrium was reached with the bulk melt. The  $\text{Ce}_2\text{O}_3/\text{CeO}_2$  ratio was determined by wet chemical analysis. A plot of  $\log P_{\text{O}_2}$  versus  $\log \left[ (\text{X}_{\text{CeO}_2})^2 / \text{X}_{\text{Ce}_2\text{O}_3} \right]$  is shown in Figure 1.

Note that the slope is approximately 2 which is expected from the following reaction:



It is possible, therefore, to estimate the equilibrium oxygen partial pressure in the bulk of the melt by noting the  $\text{Ce}_2\text{O}_3/\text{CeO}_2$  ratio. The accuracy of this method is dependent upon the assumption that equilibrium has been reached. Because a formal equilibration study was not performed, the data should be used with discretion.

### 3.3 Melting Methods

#### 3.3.1 Low Oxygen Partial Pressure Followed by Higher Oxygen Partial Pressure

Two separate melts were made where the oxygen partial pressure was increased once the glass had been melted. The results of the remelting are shown in Table 4. Melt #7 was made under severe reducing conditions (carbon crucible and  $\text{H}_2$  atmosphere) then remelted for a short time under somewhat more oxidizing conditions. The  $\text{Ce}^{+3}/\text{Ce}^{+4}$  equilibrium was shifted in favor of the  $\text{Ce}^{+3}$ . This indicates that the glass was not in equilibrium during the original melting and in subsequent melting the equilibrium was more nearly reached, although not completely.

#### 3.3.2 Constant, Low Oxygen Partial Pressure

A series of five melts were made using nitrogen or buffer gas mixtures to control the oxygen partial pressure over the melt.

This work is summarized in Table 3. Melt 6, which was made using nitrogen as a cover gas, had a high platinum content, although less than is normally experienced in commercial production. Melts 3, 4 and 5 were melted under buffer gas atmospheres having an oxygen partial pressure of  $10^{-10}$  atmosphere; their total platinum content was less than 0.033 ppm which is several orders of magnitude less than that obtained with nitrogen. The sparkler count, however, was not similarly decreased. This is attributed to the fact that, at very low oxygen partial pressures all, or nearly all, the platinum present is in the form of sparklers. Monitoring the atmosphere with the gas chromatograph during the melting cycle indicated that oxygen was evolved from the melt. The bulk glass, therefore, did not experience a constant, low oxygen partial pressure, but experienced a relatively high oxygen partial pressure followed by a low oxygen partial pressure. Such a cycle has been found to precipitate platinum sparklers as indicated in the past and elsewhere in the Report.

Chemical analysis of some incoming batch materials have revealed up to 0.080 ppm platinum. It would appear, therefore, that the platinum sparklers may have also been caused, in whole or in part, by the platinum content of initial batch materials and that platinum increase may have been negligible when melted at  $10^{-10}$  atmosphere of oxygen.

### 3.3.3 Batch Pretreatment

Several techniques were explored for pretreating the batch

in order to obtain a material that had been exposed to a low oxygen partial pressure. The pretreatments included

- a) Vacuum heating followed by melting in a 1%  $H_2$ /Argon atm.
- b) Carbon (graphite) additions
- c) Silicon additions

The purpose of the pretreatment was to remove oxygen sorbed on the batch, which was evident even when  $Ce_2(CO_3)_3$  was used in the batch instead of  $CeO_2$ . Possible sources of oxygen are absorbed water, oxygen and carbon dioxide. Oxygen sources within the batch are very serious since that oxygen is difficult to remove and can react with platinum to form  $PtO_2$  which is transported into the glass, only to decompose when the melt finally equilibrates with the controlling atmosphere. Table 2 summarizes the pretreatment melts and the conditions under which they were made. Short times were used in order to determine the effectiveness of the batch pretreatment on the initial oxygen level as indicated by the  $Ce_2O_3/CeO_2$  ratio.

Vacuum heating followed by melting in a 1%  $H_2$ /Argon atmosphere (Melt #7) was not as effective in removing oxygen from the melt as expected.  $Ce^{+3}$  was used as a starting material and some oxidation to  $Ce^{+4}$  was observed. Melt #7 dramatically indicated the propensity of the batch materials to sorb oxidized species in air and the need to add finely dispersed reduced species to the batch.

The melts where graphite or silicon were added showed an undetectable amount of  $Ce^{+4}$  indicating that the additions were effective in keeping the batch and the resultant glass at a low oxygen partial pressure. It is intended to investigate this type of pretreated batch as starting material for conventional melting

cycles with reduced atmospheres. Melt B-29 was melted under a CO/CO<sub>2</sub> buffer gas mixture. During the time the batch was introduced into the melter, substantial quantities of oxygen were also admitted so that the oxygen partial pressure at that time was many orders of magnitude above the intended 10<sup>-6</sup> atm. This glass had approximately 20,000 sparklers per cubic inch. The Ce<sup>+3</sup>/Ce<sup>+4</sup> equilibrium shows that the glass in the final stages of melting reached equilibrium with the buffer gas. The high quantity of sparklers indicates that the platinum in the glass was predominantly in the form of platinum metal particles. The remelt of B-29 under a very high oxygen partial pressure reduced the number of sparklers from 20,000 per cubic inch to 18 per cubic inch, a dramatic reduction. Laser Damage testing of the glass of melt B-29 and the remelt verified the visual microscopic examination in that many more damage sites than the approximate 20,000 per cubic inch were observed in the glass at damage energy levels of 20 joules per square centimeter. In the remelt, the number of damage sites was approximately equal to the sparkler count per cubic inch. The remelt of B-29 definitely shows that the oxidation state of platinum in the glass (metallic vs. dissolved) can be controlled by controlling the oxygen partial pressure over the melt. The high sparkler content of melt B-29 verifies the fact that once platinum oxide is dissolved in the glass in substantial quantities, it can be reduced to free platinum metal when the partial pressure of oxygen is reduced.

### 3.4 Remarks

The first experimental melts using buffer gas mixtures were done in a production melting unit. Although the total platinum content of the glass was lower than with the conventional inert atmosphere, the number of sparklers was much higher. This was attributed to the change in oxygen partial pressure during the melting cycle; when the batch was introduced into the melter, air and sorbed oxygen were also introduced. During this initial time, the platinum dissolved into the glass as a platinum oxide complex. When batch loading was completed, the  $P_{O_2}$  fell off due to the flowing buffer gas; however, the glass contained platinum dissolved into the glass as a platinum oxide complex. When batch loading was completed, the  $P_{O_2}$  fell off due to the flowing buffer gas; however, the glass contained dissolved  $PtO_2$  which then became unstable and precipitated as Pt metallic particles.

In order to counteract the relatively high  $P_{O_2}$  during the initial part of the melting cycle, crucible melts were made at low oxygen partial pressures. The introduction of air during batch loading was eliminated. The total platinum content was decreased to a very low level (20 ppb), but platinum sparklers were still present. Again, sorbed oxygen within the bulk of the melt was suspected and confirmed by gas chromatograph readings.

The next approach was to pre-treat the batch materials to remove available oxygen and then to melt at very low oxygen partial pressures. This work is still in progress. Batch pre-treatment has been found to be successful. It may also be necessary

to obtain batch materials with a lower platinum content.

Another approach yet to be tested is to subject the glass to higher oxygen partial pressures in the later stages of melting. The feasibility of this approach has already been demonstrated.

## 4. LASER FOR DAMAGE STUDIES

### 4.1 General

As discussed in previous reports, the laser to be used for damage studies should operate in the  $TEM_{00}$  mode and emit enough energy to do single shot damage testing over a relatively large area. The large oscillator-amplifier system at Owens-Illinois has been undergoing modifications to meet these criteria. With the exception of a few minor modifications, the system is in its final form. An output of 35 joules in 30 nanoseconds has been achieved. With minor changes this will be increased to more than 40 joules.

Although this 40 joule capability is not necessary for damage testing at 30 nanoseconds, it will allow, after the addition of an optical shutter, outputs of several joules at 2 nanoseconds.

### 4.2 Description of Laser

Figure 2 is a block diagram of the oscillator of the damage test laser.

Mode selection is accomplished by insertion of a 3mm diameter aperture in the cavity. This 3mm diameter is the largest usable in the present system. 3.5 mm leads to either a higher order mode or a beam cross section that departs considerably from circularity.

The 99.9% rear mirror has a 4 meter radius of curvature. The  $TEM_{00}$  mode seems slightly easier to obtain with this than with a plane mirror.

The output mirror has a 10% reflectivity. This low reflectivity is chosen in combination with the relatively long rod in this oscillator. This combination has the following desirable characteristics:

1. The  $TEM_{00}$  mode is obtained most readily when the oscillator is operating near its threshold. A longer rod, because of its better slope efficiency and lower threshold, yields a given output energy at lower pumping powers per unit length. That is, the rod can be operated near its lasing threshold and still yield sufficient output energy. Figure 3 illustrates this point. The output energy  $E_0$  is chosen so that  $E_1$  is close enough to threshold to insure  $TEM_{00}$  mode operation but far enough above threshold to insure consistency of output. ( $E_0$  fluctuates widely when  $E_1$  is too near threshold).

2. With a longer rod a lower reflectivity output mirror can be used. This results in a lower ratio of energy density inside the cavity to energy density outside the cavity, thus allowing higher output energies before damage to intercavity components occurs. In our system, with a 10% output mirror, this ratio is  $1.1/0.9 = 1.2$ .

With the 3mm diameter aperture we have obtained as much as 800 mJ in the  $TEM_{00}$  mode from the oscillator. At this level the intercavity energy density is approximately  $15 \text{ J/cm}^2$ . This is an average over space and time. Considering that the beam is gaussian in cross section, the peak energy in space can be taken as roughly twice the average energy density in space. The same thing holds temporally. Hence this 800 mJ output corresponds to

approximately  $60 \text{ j/cm}^2$  intercavity peak energy density. This is well beyond the safe operating limit and we have damaged the KD\*P of the Pockels cell and the glass of the two stacked plate polarizers. This was tracking damage. Surprisingly, no damage occurred in the glass rod. This was unexpected since KD\*P is generally considered to have a higher damage threshold than glass and because the glass rod is much longer than the KD\*P crystal.

As a consequence of this damage, the output of the oscillator is now routinely limited to a maximum of 400 mj.

The diameter of the rod in the oscillator is  $3/4$ ", but only 3 mm of this is used. This large diameter rod is used because the system is a modification of a multimode system. If this were not the case, the system would have been designed to take a smaller diameter rod. However, a large diameter does have some advantages. One of these is that thermal gradients are not as steep as in a smaller rod. Another is that a new section of the rod can easily be used in the event of damage in the lasing volume.

In routine operation this oscillator is fired no more often than once every five minutes. This has been found necessary in order to preserve the beam quality and consistency of energy output.

Figure 4 shows the amplifier section of the damage test laser. The first three amplifiers consist of  $3/4$ " x 13" (9" pumped), B/B, close wrapped rods. Pumping is accomplished by two helical flashlamps on each rod. The fourth amplifier has a 7" rod (4.5" pumped) pumped by a single helical flashlamp.

The apertures in the system are necessary to keep the beam "clean" as it passes through the system. Without these apertures there is a lot of peripheral energy around the main beam.

Lenses 1 and 2 in Figure 4 are cylindrical. They form a telescope which enlarges the beam before it is inserted into the first amplifier. The purpose of enlargement is to fill as much of the first amplifier as practicable. The purpose of rendering the beam elliptical is to make it circular after passing through the Brewster input face of the amplifier rods.

Other lenses are placed in the system to shape the beam as it passes through the amplifier chain. This is necessary because the beam becomes too large for the rods at higher pumping levels. None of these lenses are anti-reflection coated at present, so reflection losses are quite high. These lenses will be coated to prevent these losses and to prevent feedback to the oscillator.

Another loss in this system arises from Brewster angles of the rods in combination with helical flashlamps for pumping. Faraday rotation in the glass rods leads to losses at the Brewster faces. We have measured this rotation. The corresponding loss is relatively small in the subject system, but could become appreciable in other systems. Appendix II discusses this in detail. This appendix will be submitted as a paper to the Journal of Applied Optics for possible publication.

Figure 4 shows an optical shutter just before the first amplifier. This is a commercially available (Apollo Lasers) apparatus. It utilizes a laser triggered spark gap, a Pockels cell,

a Glan prism, and a high voltage power supply in its operation.

In order to match the polarization of the output from the oscillator to the polarization required in the amplifiers, the beam passes through a half wave plate before insertion into the optical shutter. After passage through this plate and through the cylindrical telescope, the beam is not sufficiently polarized to prevent appreciable leakage through the shutter. Therefore, another Glan polarizer will have to be installed after the half wave plate. Upon delivery of this polarizer and another required to replace the damaged original in the shutter, the shutter will be fully incorporated in the system.

TABLE 1.

$\text{Ce}^{+3}/\text{Ce}^{+4}$  EQUILIBRIUM AS A MEASURE OF  $\text{P}_{\text{O}_2}$

<u>MELT NO.</u>	<u><math>\text{Log P}_{\text{O}_2}</math></u> <sup>[1]</sup>	<u><math>\text{Log}(\frac{\text{X}_{\text{CeO}_2}^2}{\text{X}_{\text{Ce}_2\text{O}_3}}</math></u>
B-27	- 3.63	- 0.64
B-29	- 5.11	- 2.04
Ref. 1	- 0.68	+ 0.41
Ref. 2	- 1.55	- 0.19
Ref. 3	- 4.96	- 2.09

[1] determined with gas chromatograph

TABLE 2.

## LASER GLASS MELTS WITH ADDITIONS

MELT#	ADDITION	CRUCIBLE	ADDITION WT%	MELT TEMP. (°F)	MELT TIME (hrs.)	ATMOSPHERE	CeO <sub>2</sub> (wt%)	Ce <sub>2</sub> O <sub>3</sub> (wt%)
7	none	carbon	-	1800	1	[1]	0.151	0.42
8	graphite	"	0.27	1800	1	[1]	<0.005	0.50
9	"	"	0.54	1800	1	[1]	"	0.51
10	"	"	0.81	1800	1	[1]	"	0.48
11	"	"	1.08	1800	1	[1]	"	0.47
12	"	"	0.27	[2]	-	[1]	"	0.50
13	"	"	0.21	[3]	-	[1]	"	0.50
14	"	"	0.14	[3]	-	[1]	"	0.51
15	"	"	0.07	[3]	-	[1]	"	0.51
16	silicon	SiO <sub>2</sub>	0.20	2100	1	1% H <sub>2</sub> in A	"	0.54
17	"	"	0.10	2100	1	"	"	0.56
18	"	carbon	0.05	1800	1	[1]	"	0.52
19	"	"	0.10	1800	1	"	"	0.54
20	"	"	0.15	1800	1	"	"	0.53
21	"	"	0.20	1800	1	"	"	0.52

[1] 10<sup>-4</sup> Torr Vacuum to 1000°F then 1.0% H<sub>2</sub> in A

[2] Part of melt 8 remelted under conditions of [3]

[3] 1800°F for 165 min. then 1920°F for 15 min.

TABLE 3.

LASER GLASS MELTS AT LOW  $P_{O_2}$

MELT#	MELT TEMP. (°F)	MELT TIME (hrs.)	COVER GAS	$P_{O_2}$ (atm.)	SPARKLERS (per in <sup>3</sup> )	TOTAL Pt (ppm)	CeO <sub>2</sub> (wt%)	Ce <sub>2</sub> O <sub>3</sub> (wt%)
3	2600	21	CO/CO <sub>2</sub>	10 <sup>-10</sup>	40	0.033	<0.005	0.46
4	2600	21	H <sub>2</sub> /H <sub>2</sub> O/N <sub>2</sub>	10 <sup>-10</sup>	122	0.022	<0.005	0.47
5	2600	21	H <sub>2</sub> /H <sub>2</sub> O/N <sub>2</sub>	10 <sup>-10</sup>	42	0.017	<0.005	0.47
6	2600	21	N <sub>2</sub>	~10 <sup>-8</sup>	[1]	1.9	<0.005	0.46

[1] Partially devitrified due to slower cooling

TABLE 4.

EFFECT OF REMELTING

MELT#	MELT TEMP. (°F)	MELT TIME (hr)	COVER GAS	P <sub>O<sub>2</sub></sub> (atm)	CRUCIBLE MATERIAL	SPARKLERS (per in <sup>3</sup> )	CeO <sub>2</sub> (wt%)	Ce <sub>2</sub> O <sub>3</sub> (wt%)
7	1800	1	[1]	[2]	carbon	[3]	0.151	0.34
7(remelt)	2600	1	H <sub>2</sub> /H <sub>2</sub> O/N <sub>2</sub>	10 <sup>-10</sup>	Pt	75	0.057	0.42
B-29	2600	25.75	CO/CO <sub>2</sub>	~10 <sup>-8</sup>	Pt	~20,000	0.008	0.42
B-29 (remelt)	2600	3	O <sub>2</sub>	1.0	SiO <sub>2</sub>	18	[2]	[2]

[1] Vacuum to 1000°F then 1% H<sub>2</sub> in A

[2] Not determined

[3] Too seedy to analyze

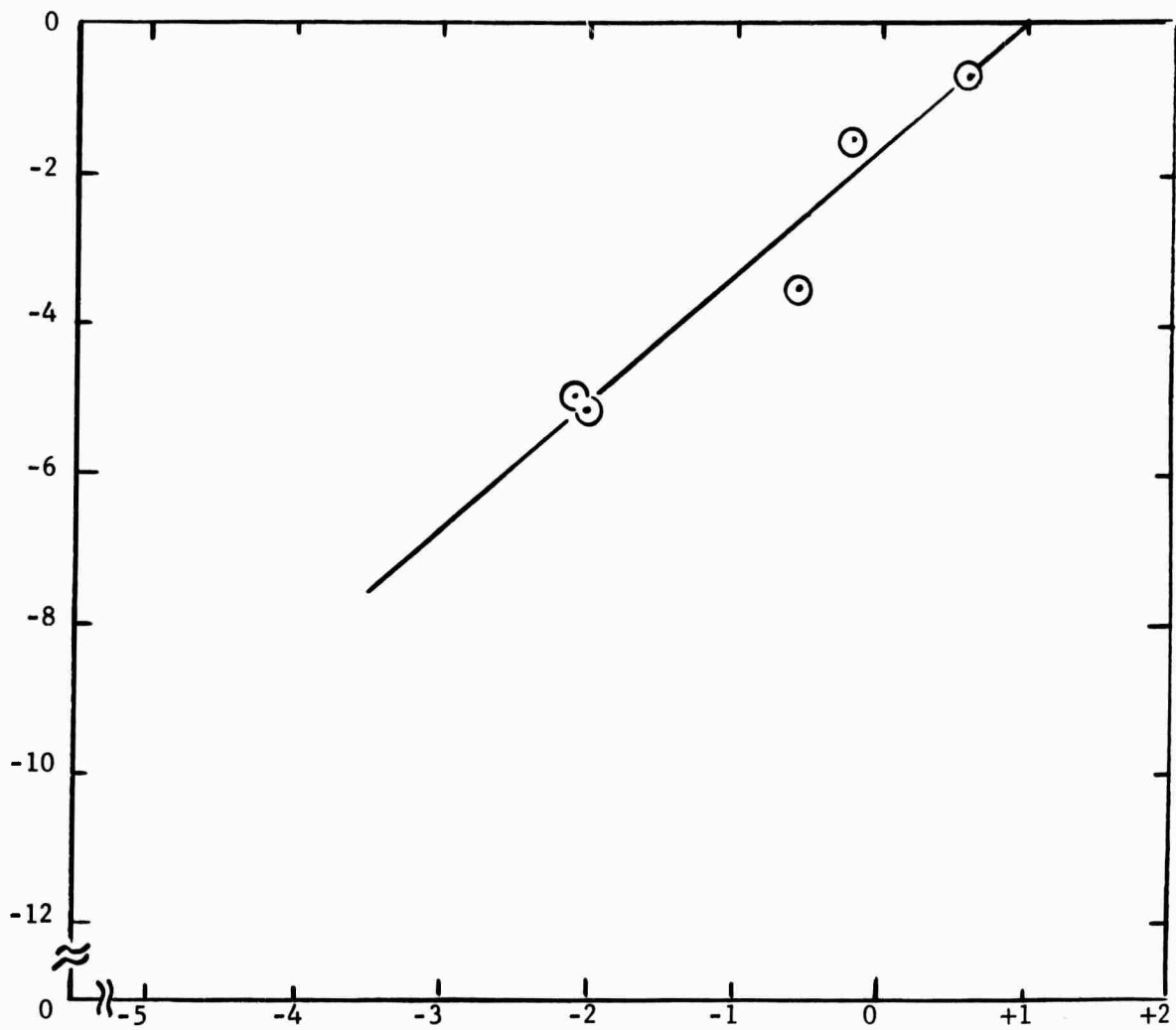
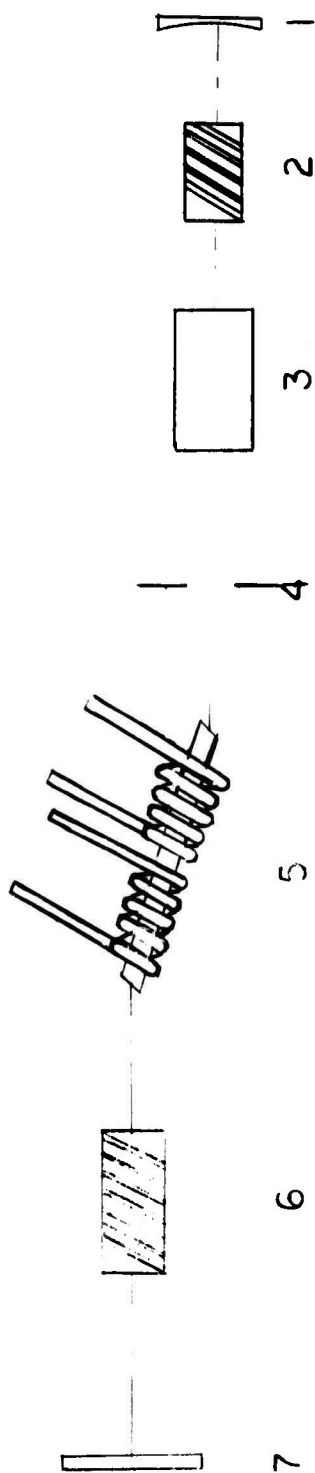


FIG. 1.  $\text{Log}(X_{\text{CeO}_2})^2 / X_{\text{Ce}_2\text{O}_3}$  vs  $\text{Log } P_{O_2}$  for **laser** glass melted under different oxygen partial pressures.



- 1 Rear mirror - 4 meter radius curvature
- 2 Stacked plate polarizer
- 3 Pockel's cell
- 4 3 mm diameter aperture
- 5 13x3/4 inch Brewster - Brewster rod
- 6 Stacked plate polarizer
- 7 10% reflectivity output mirror

FIGURE 2 OSCILLATOR

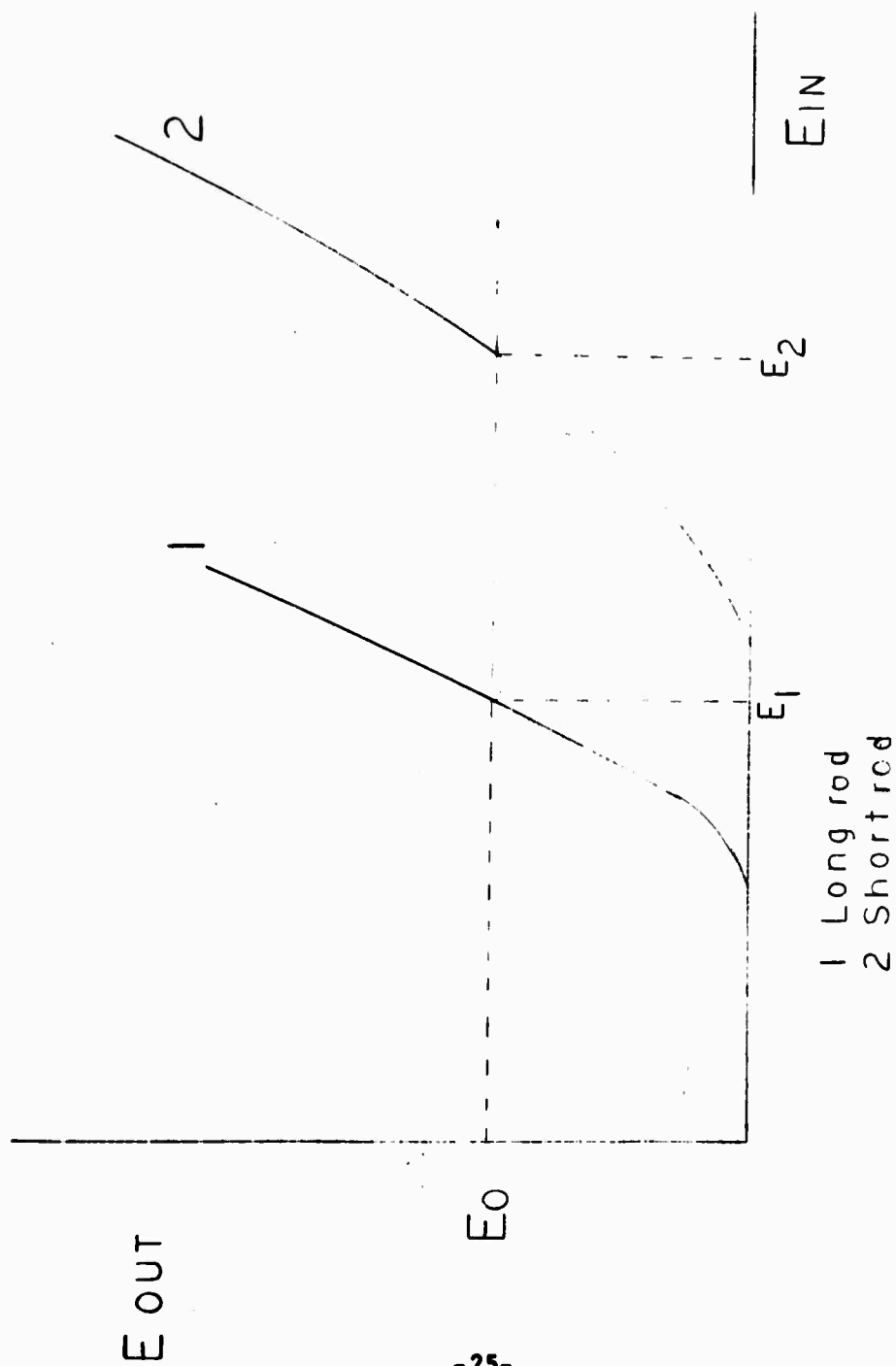
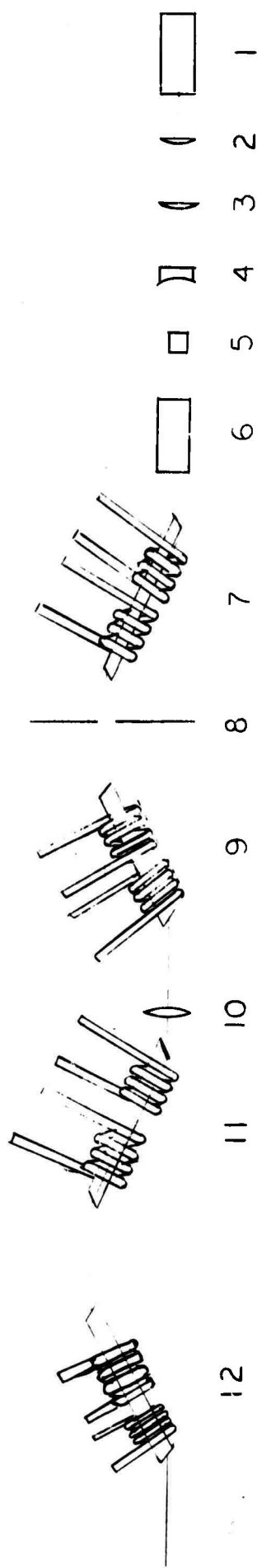


FIGURE 3 ILLUSTRATION OF ADVANTAGES OF LONG ROD OVER SHORTER ROD FOR USE IN TEM<sub>00</sub> MODE OSILLATORS



1. OSCILLATOR
- 2 & 3. CYLINDRICAL LENS
4. SPHERICAL EXPANDING LENS
5. HALF WAVE PLATE
6. OPTICAL SHUTTER
7. 1.3X 3/4 INCH BREWSTER-BREWSTER AMPLIFIER
8. APERTURE
9. 1.3X 3/4 INCH BREWSTER-BREWSTER AMPLIFIER
10. SPHERICAL CONVERGING LENS
- 11 & 12. 1.3X 3/4 INCH BREWSTER-BREWSTER AMPLIFIER

FIGURE 4 OSCILLATOR-AMPLIFIER SYSTEM

## APPENDIX I

### Ce<sup>+3</sup>/Ce<sup>+4</sup> EQUILIBRIUM

Consider the reaction



The standard state free energy change for the reaction can be written as follows

$$\Delta F^\circ_{1700^\circ\text{K}} = -RT \ln \frac{a_{\text{Ce}_2\text{O}_3} P_{\text{O}_2}^{\frac{1}{2}}}{(a_{\text{CeO}_2})^2}$$

where  $\Delta F^\circ$  = standard state free energy change for the reaction in calories per mole

R = gas constant 1.987 cal/mole/ $^\circ\text{K}$

a = activity

P = partial pressure

substituting  $X\gamma = a$  where

X = mole fraction

$\gamma$  = activity coefficient

$$\Delta F^\circ_{1700^\circ\text{K}} = -RT \ln \frac{X_{\text{Ce}_2\text{O}_3}}{(X_{\text{CeO}_2})^2} - RT \ln \frac{\gamma_{\text{Ce}_2\text{O}_3}}{(\gamma_{\text{CeO}_2})^2} - RT \ln P_{\text{O}_2}^{\frac{1}{2}}$$

assuming that the activity coefficient is constant at constant temperature

$$- \frac{\Delta F^\circ_{1700^\circ\text{K}}}{RT} - \ln \frac{\gamma_{\text{Ce}_2\text{O}_3}}{(\gamma_{\text{CeO}_2})^2} = \text{constant}$$

then

$$\frac{1}{2} \ln P_{\text{O}_2} = \ln \frac{(X_{\text{CeO}_2})^2}{X_{\text{Ce}_2\text{O}_3}} + C$$

or

$$\ln P_{\text{O}_2} = 2 \ln \frac{(X_{\text{CeO}_2})^2}{X_{\text{Ce}_2\text{O}_3}} + 2C$$

The molecular weight of the glass is 54.023 grams per mole. The values of

$X_{\text{Ce}_2\text{O}_3}$  and  $X_{\text{CeO}_2}$  can then be calculated. A plot of  $\ln P_{\text{O}_2}$  vs  $\ln(X_{\text{CeO}_2})^2/X_{\text{Ce}_2\text{O}_3}$

should yield a straight line with a slope of 2.

**APPENDIX II**

**FARADAY ROTATION IN Nd:GLASS LASER SYSTEMS**

**by**

**G. Dube' and N. L. Boling**

**Owens-Illinois, Inc.**

**Toledo, Ohio 43607**

# **ABSTRACT**

Faraday rotation in Nd:glass laser rods pumped by helical flashlamps is predicted and experimentally measured. Some consequences of this rotation are considered, and methods for eliminating its adverse effects are suggested and demonstrated.

Many high-power laser systems use a string of Nd:glass laser rod amplifiers. Frequently the input pulse to these amplifiers is linearly polarized and the amplifier rods (and other components) have Brewster angle entrance and exit faces to reduce reflection losses. If helical flashlamps pump these rods, an appreciable magnetic field is created along the axis of the laser rod. This magnetic field is due to the intense current flowing through the solenoid-like flashlamps. Field strengths in the kilo-Oersted region are not uncommon. Nd:glass, like most materials, exhibits Faraday rotation in the presence of a magnetic field.<sup>1</sup> The magnitude and consequences of this rotation of the plane of polarization are considered.

If the plane of polarization is rotated, the reflection losses at each of the formerly Brewster angle surfaces will increase. This reduces the apparent gain and output of the laser amplifier system. These losses can be significant if the output of several laser amplifier rods is further amplified by a Brewster angle disk laser. This pump-induced Faraday rotation may partially account for observed "anomalous" reductions in gain at high pumping intensities.<sup>2</sup> Reversing the polarity (direction of current flow) of half of the helical flashlamps reduces the Faraday rotation. If an even number of identical helical flashlamps are used, the net rotation should be reduced to zero.

We used the experiment indicated in Figure 1 to demonstrate and measure the Faraday rotation. Each amplifier contained two helical flashlamps that pumped 20 cm of a 30 cm long Nd:glass rod. A He-Ne laser ( $\lambda \approx .63 \mu\text{m}$ ) was used. At this wavelength we have measured the Verdet constant ( $V$ )<sup>1</sup> of this laser glass (Owens-Illinois ED-2) to be approximately .0116 min/Oe-cm. The Verdet constant (and Faraday rotation) at  $1.06 \mu\text{m}$  should be about one-third of the .63  $\mu\text{m}$  value.<sup>3,4</sup> Each of the oscilloscope traces in Figure 2 shows three sweeps. The lowest straight line is the zero level reference. The other straight line is the photodetector response to the transmission of the He-Ne light through the polarizer-amplifier-analyzer system before the amplifier flashlamps are fired. The third sweep is triggered when the flashlamps are triggered and indicates the transmission of the He-Ne light during the flashlamp pulse. With the polarizer and analyzer parallel there is no significant change in transmission during the flashlamp pulse (which peaks approximately 250  $\mu\text{s}$  after triggering). After the flashlamp pulse, thermal distortions enlarge the beam so the transmission through the small apertures is decreased. The beam was closely apertured to reduce the amount of flashlamp light reaching the detector.

In Figure 2a the analyzer was rotated  $60^\circ$  to the right, and the transmitted signal increased during the flashlamp pulse; indicating that the plane of polarization was rotated in that direction (to the right or opposite to the current flow through the flashlamps).

In Figure 2b the analyzer was rotated  $60^\circ$  to the left and the transmission decreased during the flashlamp pulse, as expected. This indicates to us that Faraday rotation, not stress induced birefringence, is responsible for the observed changes in transmission.

To determine the amount of rotation, the transmission before and during the flashlamp pulse was recorded at different analyzer settings. Figure 3 shows the result. The curves are not  $\cos^2$  curves because of detection system nonlinearities. The indicated rotation ( $\theta$ ) is approximately  $11^\circ$ . Theoretically  $\theta$  is given by<sup>1</sup>

$$\theta = V \int_0^1 H(x) dx \approx VHl \quad \text{Eq. 1}$$

where  $H(x)$  is the magnetic field strength and  $l$  is the length of the field (or material). The magnetic field strength (Oersteds) at the center of one turn of the flashlamp coil is given by<sup>5</sup>

$$H = \frac{2\pi}{10} \frac{I}{r} \quad \text{Eq. 2}$$

where  $I$  is the current (amperes) and  $r$  is the radius (cm) of the coil. The peak current through the flashlamp is approximately given by

$$I \approx \frac{Q}{\tau} = \frac{CV}{\tau} \quad \text{Eq. 3}$$

where  $\tau$  is the half-width of the flashlamp pulse ( $\approx 400 \mu s$  in our case),  $C$  is the capacitance ( $3.3 \times 10^{-4}$  fd), and  $Q$  and  $V$  are, respectively, the charge and voltage ( $5.6 \times 10^3 V$ ) of the capacitors.

Using these values we have

$$\theta = V l \frac{2\pi}{10} \frac{1}{r} \frac{CV}{\tau} = 671 \text{ minutes} \approx 11.2^\circ \quad \text{Eq. 4}$$

in good agreement with the observed rotation.

Next the polarity of half of the flashlamps was reversed and the analyzer was again set at  $60^\circ$  to the right (and left) of the parallel position. Figures 2c (and 2d) show that the transmission now remained nearly constant during the flashlamp pulse. Little, if any, Faraday rotation was evident when the polarity of half of the flashlamp was reversed. A small rotation should remain if the flashlamp currents are not all equal, due to the reversed polarity or inherent flashlamp differences.

Now we consider the losses resulting from a Faraday rotation of  $\theta$ , neglecting birefringence and any other complicating effects. If the incident light is 100% "p" polarized,<sup>6</sup> a rotation of  $\theta$  reduces the "p" intensity to  $I_0 \cos^2 \theta$  and creates an "s" intensity  $I_0 \sin^2 \theta$  where  $I_0$  is the initial "p" intensity. If polarizers are used between amplifiers (as isolators, shutters, etc.) their transmission is reduced by  $\cos^2 \theta$ . The transmission (T) through N formerly Brewster angle surfaces can be written as

$$T = \cos^2 \theta + (1 - R_s)^N \sin^2 \theta \quad \text{Eq. 5}$$

where  $R_s$  is the reflectivity of the "s" polarization at Brewster's angle. For a typical Brewster angle disk laser amplifier  $N \approx 16$  (8 disks) and  $R_s \approx .17$  (refractive index 1.55). For a  $\theta$  of  $10^\circ$  and  $20^\circ$  we have a transmission of .97 and .89 (reflection losses of 3% and 11%), respectively. These losses can easily be avoided and should not be neglected in the design of high power laser systems.

In some cases (a small oscillator for instance) only one helical flashlamp is used, so reversing the polarity of half the

flashlamps is impossible. If a polarization dependent Q-switch is used, Faraday rotation could increase the leakage or prelasing characteristics of the oscillator. By properly choosing the Nd concentration, and using a host material with a V opposite in sign to the V of the Nd, it may be possible to produce a Nd:glass material with a Verdet constant of zero.<sup>7</sup>

If lasing materials with large Verdet constants could be made, it might be advantageous to design systems in which one rod serves as both a laser amplifier and a Faraday isolator.<sup>8</sup> We are continuing to study these and other implications of Faraday rotation in laser (and other) materials.

## REFERENCES

1. F. A. Jenkins and H. E. White, Fundamentals of Optics (New York: McGraw-Hill, 1957), p.596.
2. T. H. DeRieux and J. M. McMahon, "Laser Glass Testing at NRL," Damage in Laser Materials, National Bureau of Standards Special Publication 341, ed. A. Guenther and A. Glass (Washington, D.C., U.S. Government Printing Office, 1970), pp. 19-27.
3. N. F. Borrelli, "Faraday Rotation in Glasses," J. Chem. Phys., Vol. 41, pp. 3289-3293, 1 December 1964.
4. C. B. Rubinstein, S. B. Berger, L. G. VanViert, and W. A. Bonner, "Faraday Rotation of Rare-Earth (III) Borate Glasses," J. Appl. Phys., Vol. 35, pp. 2338-2340, August 1964.
5. Handbook of Chemistry and Physics, ed. C. D. Hodgman, R. T. Weast, and S. M. Selby, (Cleveland, Ohio: Chemical Rubber Publishing Co., 1960), p. 3105.
6. F. A. Jenkins and H. E. White, op. cit., ch.25.
7. C. G. Robinson and R. E. Graf, "Faraday Rotation in Praseodymium, Terbium, and Dysprosium Alumina Silicate Glasses," Appl. Opt., Vol. 3, pp. 1190-1191, October 1964.
8. B. A. Lengyel, Lasers, second edition (New York: Wiley-Interscience, 1971), pp. 179-182.

# FIGURE CAPTIONS

Figure 1. Experimental Arrangement for Observing Pump Induced Faraday Rotation

Figure 2. Transmitted Intensity (Arbitrary Scale) Versus Time (100  $\mu$ s/division). (a) and (b), All Flashlamps with the same Polarity; (c) and (d), Half of the Flashlamps with Reversed Polarity.

Figure 3. Transmitted Intensity (Arbitrary Scale) Versus Analyzer Setting (degrees). Analyzer and Polarizer Parallel at 0°.

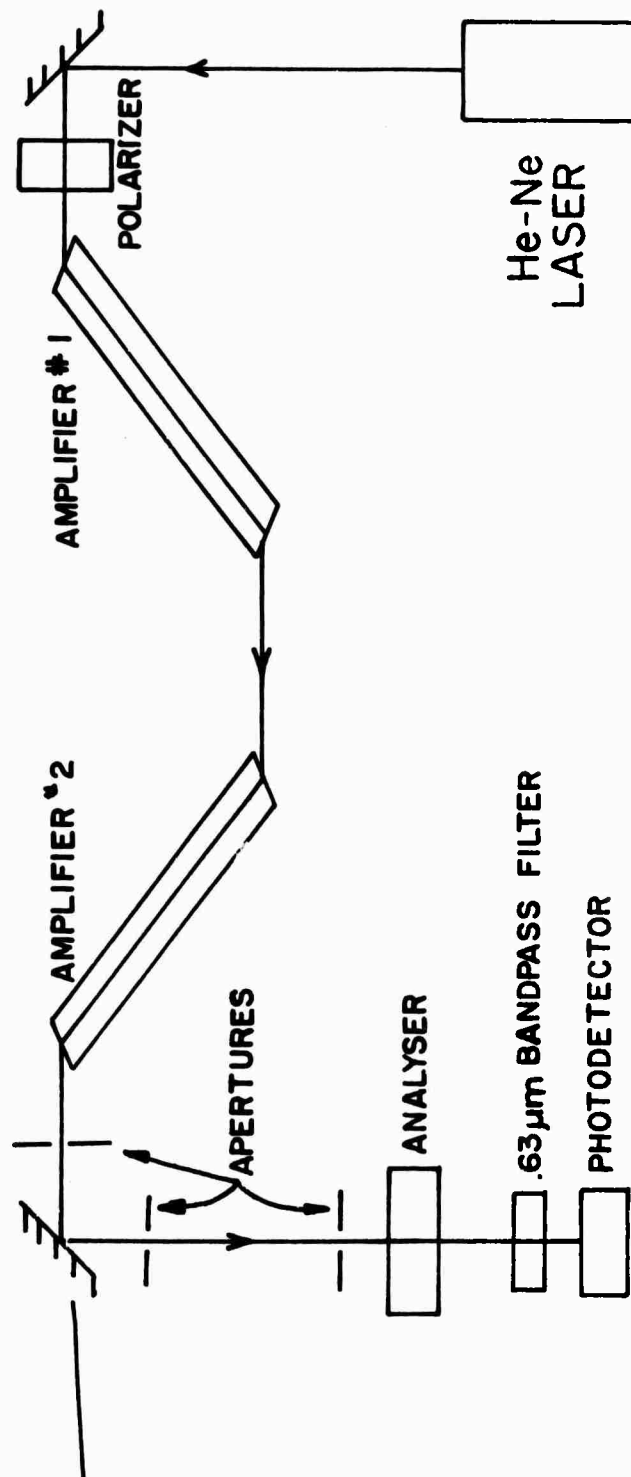
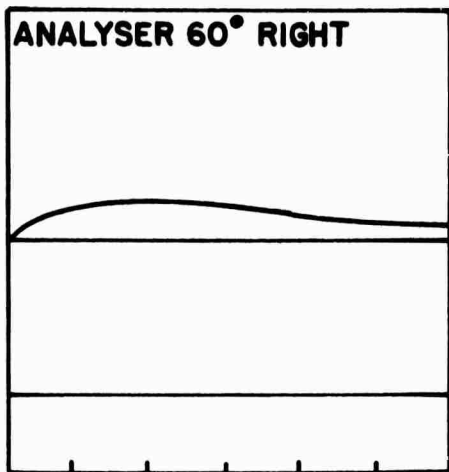
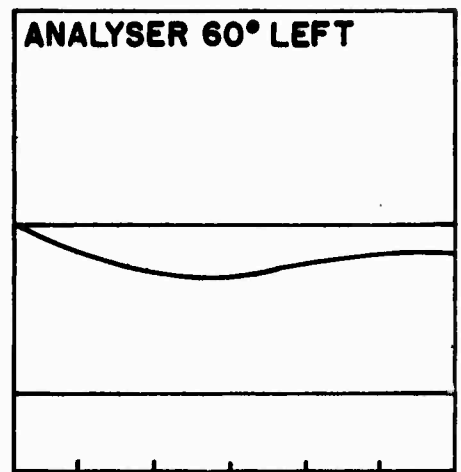


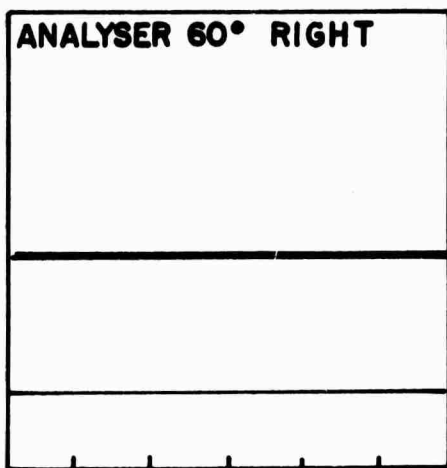
FIGURE 1 - (APPENDIX II)



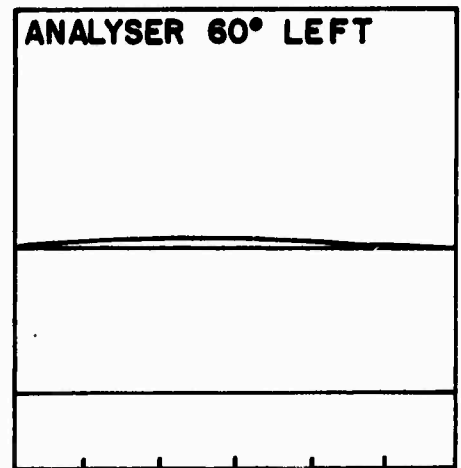
(a)



(b)

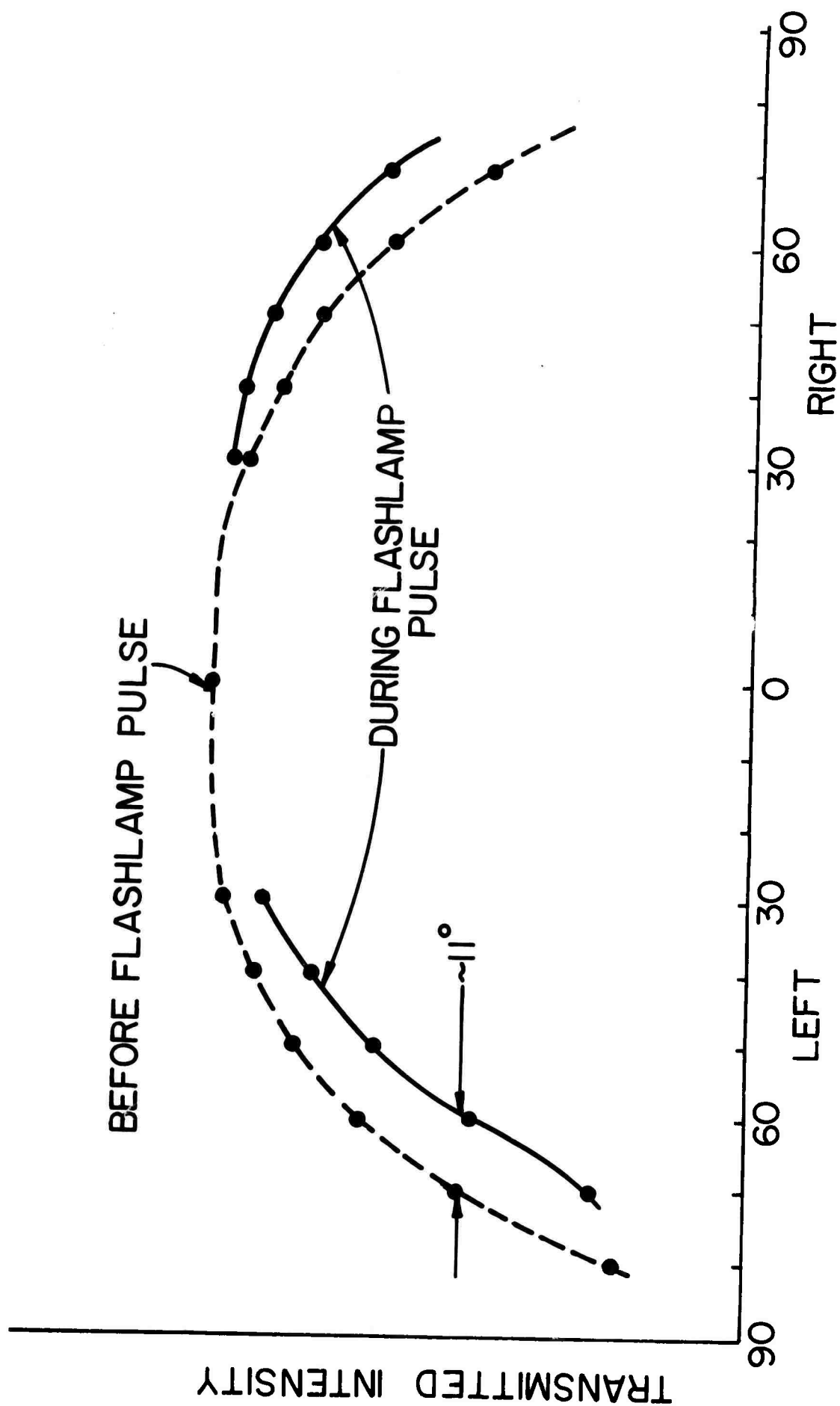


(c)



(d)

**FIGURE 2 - (APPENDIX II)**



ANALYSER SETTING (DEGREES)

FIGURE 3 (APPENDIX II)